S. Glaßer*, P. Berg, S. Voß, S. Serowy, G. Janiga, B. Preim, O. Beuing

From Imaging to Hemodynamics – How Reconstruction Kernels Influence the Blood Flow Predictions in Intracranial Aneurysms

Abstract: Computational Fluid Dynamics is increasingly used by biomedical engineering groups to understand and predict the blood flow within intracranial aneurysms and support the physician during therapy planning. However, due to various simplifications, its acceptance remains limited within the medical community.

To quantify the influence of the reconstruction kernels employed for reconstructing 3D images from rotational angiography data, different kernels are applied to four datasets with patient-specific intracranial aneurysms. Sharp, normal and smooth reconstructions were evaluated. Differences of the resulting 24 segmentations and the impact on the hemodynamic predictions are quantified to provide insights into the expected error ranges. A comparison of the segmentations yields strong differences regarding vessel branches and diameters. Further, sharp kernels lead to smaller ostium areas than smooth ones. Analyses of hemodynamic predictions reveal a clear time and space dependency, while mean velocity deviations range from 3.9 % to 8 %.

The results reveal a strong influence of reconstruction kernels on geometrical aneurysm models and the subsequent hemodynamic parameters. Thus, patient-specific blood flow predictions require a carefully selected reconstruction kernel and appropriate recommendations need to be formulated.

Keywords: Computational Fluid Dynamics, Hemodynamics, Intracranial aneurysm, Reconstruction

DOI 10.1515/abc-YYYY-XXXX

***corresponding author: S. Glaßer:** Department of Simulation and Graphics, University of Magdeburg, Germany, e-mail: glasser@ovgu.de

P. Berg, S. Voß, G. Janiga: Department of Fluid Dynamics and Technical Flows, University of Magdeburg, Germany, e-mail: berg@ovgu.de, samuel.voss@ovgu.de, janiga@ovgu.de

B. Preim: Department of Simulation and Graphics, University of Magdeburg, Germany, e-mail: preim@ovgu.de

S. Serowy, O. Beuing: Department of Neuroradiology, University Hospital Magdeburg, Germany, e-mail: serowy@med.ovgu.de, beuing@med.ovgu.de

1 Introduction

Within the last decades, Computational Fluid Dynamics (CFD) has been increasingly used to predict blood flow in intracranial aneurysms (IAs). Studies of large cohorts of patient-specific dilatations mainly try to understand initiation, remodelling as well as rupture processes in order to assist physicians during therapy planning [1,2]. However, due to several assumptions, which are required to receive numerical results in a feasible time frame, the acceptance of CFD remains limited in the clinical context.

Therefore, several groups mainly focused on the evaluation of the variability of hemodynamic predictions based on varying input parameters. Berg et al. [3] compared in a double-blinded, international CFD challenge numerical solutions of 28 participating groups for two patient-specific IAs under given boundary conditions. The results were in a good agreement with only few outliers due to invalidated solvers or inadvertence during post-processing. To quantify the impact of geometry, Szikora et al. [4] simulated the blood flow in 21 IAs. They concluded that IAs with a main axis parallel to the parent artery are more prone to rupture than those with a perpendicular axis. Geers et al. [5] compared computer tomographic angiography and 3D rotational angiography (RA) images to evaluate the reproducibility of computational hemodynamics in IAs. As a result, different imaging modalities lead to equivalent predictions of the main flow characteristics, but large discrepancies in quantitative measurements are present.

This study extends the usual workflow and incorporates the reconstruction process directly from the digital subtraction angiography (DSA) suite Artis Q (Siemens Healthcare GmbH, Forchheim, Germany). Four patient-specific IA data sets are reconstructed with six available kernels. Next, 24 configurations are segmented and analysed regarding the IAs' morphology and the impact on blood flow prediction.

2 Materials and Methods

2.1 Case description

Four IAs in four female patients with mean age of 50 years (range 45-59 years) were investigated in this study. Three cases exhibit acute subarachnoid hemorrhage (SAH), and one aneurysm was incidentally found. Clinical condition was poor in two of the patients with acute SAH (grade IV according to Hunt and Hess), the other two patients had no significant neurologic deficits. One IA was located at the anterior communicating artery, one at the posterior communicating artery, one at the segment of the internal carotid artery, and one at the bifurcation of the middle cerebral artery. Their size varied from approximately 2.5 mm to 8.0 mm. All IAs were treated with endovascular coiling.

2.2 Reconstruction and segmentation

From the RA image data, 6 3D-DSA images were reconstructed per patient by using the kernels EE (edge enhanced) smooth, EE normal, EE sharp, HU (Hounsfield unit) smooth, HU normal and HU sharp. This results in a total number of 24 configurations.

For each patient, a threshold-based segmentation, as proposed in [6], was carried out for the HU normal reconstructed DSA image data. Next, the remaining reconstructions of the same patient were carried out such that they exhibit similar contours in a representative slice covering the aneurysm, see Fig. 1. Based on each threshold, the iso-surface is extracted to obtain the triangle surface mesh.

2.3 Clinical research prototype

The hemodynamic simulations were carried out with a clinical research prototype. To define the cross-sections where in- and outflow boundary conditions are applied, the vessel surfaces were cropped. A time-dependent velocity profile corresponding to a measured flow curve was defined at the inlet and zero-pressure conditions were set at the outlet cross sections. All required settings of the Lattice-Boltzmann solver were pre-defined and could be adjusted by experienced users. Blood was treated as an incompressible (ρ=1000 kg/m^3), Newtonian (η=4 mPa·s), laminar fluid and rigid walls were assumed. By default, two cardiac cycles were simulated, whereas only the second one was considered. To guarantee an appropriate mesh resolution, an element size of approximately 0.1 to 0.15 mm was chosen, yielding a coverage of the minimum ostium diameter by at least 20 voxels. Due to the efficient parallelization of the GPU-based solver, computational times of the unsteady simulations were approximately 30 to 45 minutes per case.

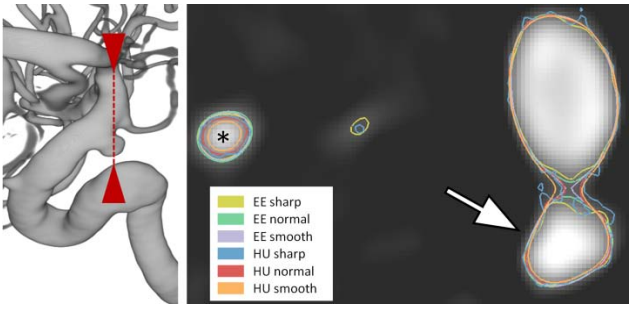

Figure 1: To provide comparable segmentations, a slice with the aneurysm of patient VA (indicated with arrowheads, left) is chosen. A threshold is selected such that similar IA segmentations are achieved (see arrow, right). The resulting segmentation masks are color-coded. The reconstruction kernels influence the extent of the segmentation, especially for peripheral vessels (see *, right).

2.4 Qualitative and quantitative analyses

For a qualitative analysis of the segmented aneurysm models, a simultaneous view of all six surfaces was implemented in MeVisLab 2.8 (MeVis Medical Solutions AG, Bremen, Germany, www.mevislab.de), a tool for medical image processing and visualization, see Fig. 2. A transparent shading technique allows for an interactive and combined exploration of the vessel models.

Furthermore, the effect of different segmentations on the subsequent hemodynamic computations was evaluated using centrelines for the velocity fields. In this regard, spatial and temporal influences are considered and the variability of numerical predictions is quantified.

3 Results

3.1 Segmentation results

A 3D view of the segmented IA models is provided in Fig. 2. The qualitative analysis revealed the missing of small vessels for smooth and normal reconstructions. Even for larger vessel parts, including the aneurysm neck, segmentations based on sharp reconstructions yield larger diameters. Although the segmentation threshold was carefully adapted such that similar aneurysm head segmentations were obtained, the aneurysm volume decreases from sharp to normal to smooth reconstructions.

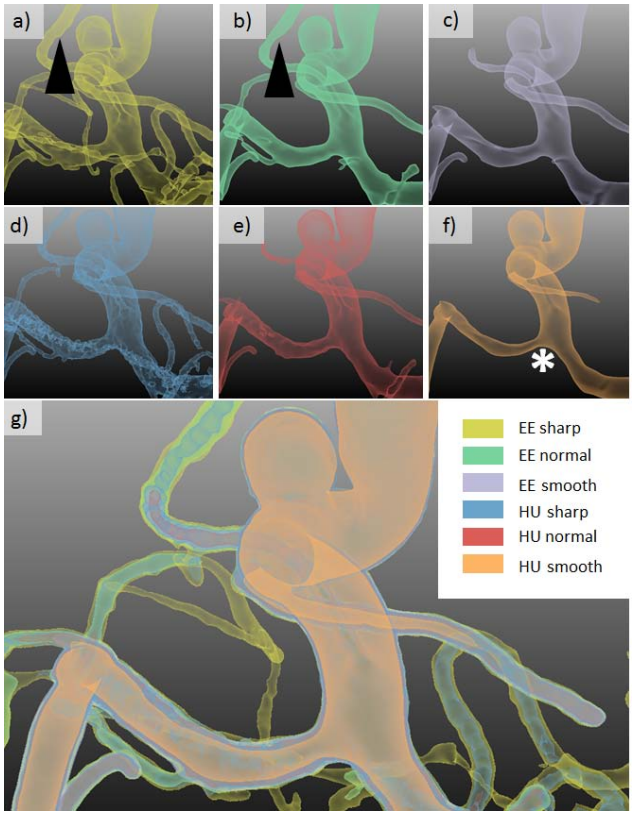

Figure 2: a)-f) Transparent, shaded 3D surface views for the six segmentation results for case EM including bifurcations (*) and peripheral vessels (arrowheads). g) Combined view of all segmentations.

Comparison of HU smooth and EE smooth indicates a slightly better result regarding bifurcations (see the example marked with * in Fig. 2e). Furthermore, branching vessels next to the aneurysm are better preserved in the EE-based segmentations (see arrowheads in Fig. 2a and b).

For comparison of the aneurysm's inflow zone, the ostium was approximated as intersecting plane dividing the aneurysm from the parent vessel. The resulting areas are compared in Fig. 3. Hence, segmentations based on smooth reconstruction kernels yielded larger ostium areas, whereas segmentations based on sharp reconstruction kernels resulted in smaller ostium areas.

3.2 Hemodynamic predictions

The effect of different reconstruction kernels on the hemodynamic predictions is exemplarily illustrated in Fig. 4 for case MD. The velocity magnitude along the centreline shows a good agreement in the proximal part of the investigated domain. However, the numerical predictions strongly deviate in the distal part, especially between EE and HU. An equivalent behaviour is observed for the pressure predictions (not presented here).

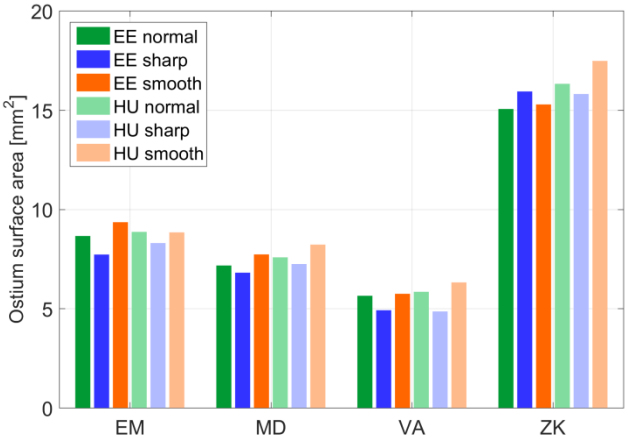

Figure 3: Ostium surface areas for the four patients and six segmentation results.

To quantify the effect of time-dependency, Table 2 contains the standard deviations normalized to mean values for the four aneurysms at ten time steps over the cardiac cycle. It can be noticed that with increasing inflow velocity the deviations increase with the highest differences at peak-systole. However, the overall differences of the velocity results remain relatively low compared to the strong geometric deviations presented earlier.

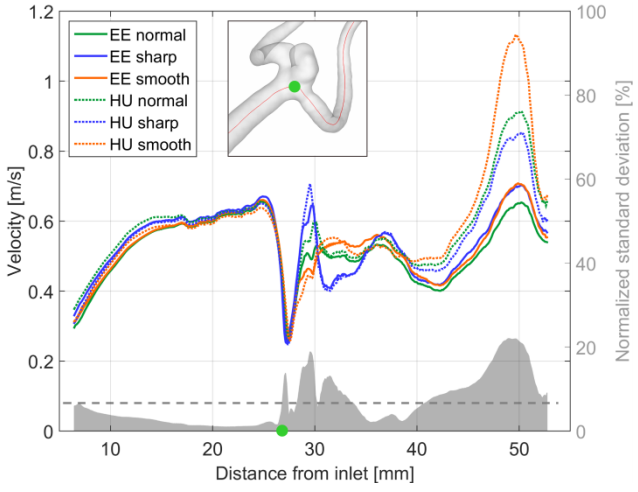

Figure 4: Velocity prediction along the centreline of case MD for the six different reconstruction kernels at one time step (top). Location-dependent normalized standard deviation (SD) illustrated in grey with the mean value presented by a dashed line (bottom).

Table 2: Normalized standard deviation for centreline velocity at 10 time steps. Highest values are bold. * indicates that EE sharp is not considered due to unsuccessful simulations.

Case	Normalized standard deviation [%] over time									
	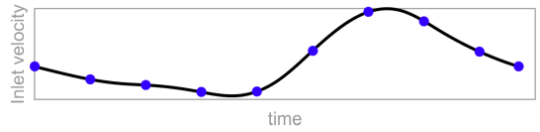									
EM	4.0	5.9	3.9	3.9	3.9	4.2	**5.2**	5.1	4.5	4.2
MD	6.1	6.0	5.8	5.7	5.9	6.4	**6.7**	6.5	6.2	6.1
VA*	6.5	5.9	5.5	5.3	4.6	5.8	7.3	**8.0**	7.0	6.7
ZK*	6.0	5.9	5.8	5.8	5.8	6.1	6.3	**6.4**	6.2	6.1

4 Discussion

The qualitative comparison of the segmentations based on the six reconstruction kernels yields strong differences regarding branching vessels as well as vessel diameters. Sharp kernels tend to produce noisy surfaces, which are not well-suited for simulation. Smooth kernels yield smoother surfaces but are usually accompanied with smaller vessel cross-sections. Furthermore, segmentations based on EE kernels better comprise surrounding vessels and avoid a decrease in the vessel diameter at bifurcations. When analysing quantitative segmentation results, sharp kernels mostly lead to smaller and smooth kernels to larger ostium areas, respectively. Smooth kernels shrink elongated structures like small vessels, but flatten regions with high curvature, and thus increase the neck area. Sharp kernels yield opposite effects.

Equivalent observations are present with respect to the hemodynamic computations. Although the velocity values were in a good agreement in some vessel sections, other regions in the investigated domains clearly depend on the results of the reconstruction kernel. Hence, the results demonstrate how sensitive hemodynamic parameters depend on geometric variations. This awareness should lead to a careful selection of reconstruction kernels, if CFD computations and therefore patient-specific blood flow predictions are desired. As a result, we strongly recommend including the influence of reconstruction kernels into future CFD challenges like the challenge presented in [3].

Within this study the following limitations need to be mentioned: Firstly, the segmentations are based on a global threshold and a locally adapted segmentation may improve the quality of the 3D surface meshes. Secondly, the hemodynamic simulations assume rigid vessel walls without considering fluid-structure interactions. Thirdly, due to the lack of patient-specific boundary conditions, a representative flow curve was applied.

Acknowledgment: The authors warmly acknowledge Dr. Thomas Redel (Siemens Healthcare GmbH, Forchheim, Germany) for his support regarding the clinical research prototype. Further, we thank Marko Bögel (Friedrich-Alexander-University Erlangen-Nürnberg), who supported the segmentation process with fruitful discussions.

Funding: This work was partly funded by the Federal Ministry of Education and Research in Germany within the Research Campus *STIMULATE* (grant no. 03FO16102A).

Author's Statement

Conflict of interest: Authors state no conflict of interest. Material and Methods: Informed consent: Informed consent has been obtained from all individuals included in this study. Ethical approval: The research related to human use has been complied with all the relevant national regulations, institutional policies and in accordance the tenets of the Helsinki Declaration, and has been approved by the authors' institutional review board or equivalent committee.

References

[1] Xiang J, Natarajan SK, Tremmel M et al. Hemodynamic-morphologic discriminants for intracranial aneurysm rupture. Stroke 2011; 42:144-52.

[2] Cebral JR, Mut F, Weir J et al. Association of Hemodynamic Characteristics and Cerebral Aneurysm Rupture. American Journal of Neuroradiology 2011; 32: 264-270.

[3] Berg P, Roloff C, Beuing O et al. The Computational Fluid Dynamics Rupture Challenge 2013 – Phase II: Variability of hemodynamic simulations in two intracranial aneurysms. Journal of Biomechanical Engineering 2015; 137: 121008/1-13.

[4] Szikora I, Paal G, Ugron A et al. Impact of aneurysmal geometry on intraaneurysmal flow: a computerized flow simulation study. Interventional Neuroradiology 2008; 50: 411–421.

[5] Geers AJ, Larrabide I, Radaelli G et al. Reproducibility of image-based computational hemodynamics in intracranial aneurysms: Comparison of CTA and 3DRA. Proc IEEE International Symposium on Biomedical Imaging: From Nano to Macro 2009; 610–613.

[6] Glaßer S, Berg P, Neugebauer M et al. Reconstruction of 3D surface meshes for blood flow simulations of intracranial aneurysms. Proc of Computer- und Roboterassistierte Chirurgie (CURA) 2015; 163-169.